

# Generic searches for alternative gravitational wave polarizations with networks of interferometric detectors

Peter T. H. Pang,<sup>1, 2,\*</sup> Rico K. L. Lo,<sup>3, †</sup> Isaac C. F. Wong,<sup>4, ‡</sup> Tjonne G. F. Li,<sup>4</sup> and Chris Van Den Broeck<sup>1, 2</sup>

<sup>1</sup>*Nikhef – National Institute for Subatomic Physics,  
Science Park, 1098 XG Amsterdam, The Netherlands*

<sup>2</sup>*Department of Physics, Utrecht University, Princetonplein 1, 3584 CC Utrecht, The Netherlands*

<sup>3</sup>*LIGO, California Institute of Technology, Pasadena, California 91125, USA*

<sup>4</sup>*Department of Physics, The Chinese University of Hong Kong, Shatin, N.T., Hong Kong*

The detection of gravitational wave signals by Advanced LIGO and Advanced Virgo enables us to probe the polarization content of gravitational waves. In general relativity, only tensor modes are present, while in a variety of alternative theories one can also have vector or scalar modes. Recently tests were performed which compared Bayesian evidences for the hypotheses that either purely tensor, purely vector, or purely scalar polarizations were present. Indeed, with only three detectors in a network and allowing for *mixtures* of tensor polarizations and alternative polarization states, it is not possible to identify precisely which non-standard polarizations might be in the signal and by what amounts. However, we demonstrate that one can still infer whether, in addition to tensor polarizations, alternative polarizations are present in the first place, irrespective of the detailed polarization content. We develop two methods to do this for sources with electromagnetic counterparts, both based on the so-called null stream. Apart from being able to detect mixtures of tensor and alternative polarizations, these have the added advantage that no waveform models are needed, and signals from any kind of transient source can be used. Both formalisms allow us to combine information from multiple sources so as to arrive at increasingly more stringent bounds. For now we apply these on the binary neutron star signal GW170817, showing consistency with the tensor-only hypothesis with p-values of 0.315 and 0.790 for the two methods.

## I. INTRODUCTION

Since 2015, the Advanced LIGO [1] and Advanced Virgo [2] have been detecting gravitational wave (GW) signals on a regular basis [3–11]. This has enabled a variety of tests of general relativity (GR), including but not limited to the strong-field dynamics of binary coalescence [12–15], the way GWs propagate over large distances [6, 14, 16], and preliminary investigations into their polarization content [9, 15, 17].

Generic metric theories of gravity allow for the existence of up to six GW polarization states for gravitational waves [18], which can be categorized into tensor modes, vector modes, and scalar modes. While GR only permits the tensor modes, some theories of gravity predict additional polarizations; see e.g. [19] and references therein. In [9, 12, 15, 17], ratios of Bayesian evidences were computed for the hypotheses that only tensor polarizations, only vector polarizations, or only scalar polarizations were present in the signals. Yet, in realistic alternative theories of gravity, typically *mixtures* occur of tensor modes together with vector and/or scalar polarization states.

In this paper we develop methodology that will allow us to check for the existence of such mixtures, in GW signals from sources whose exact sky position is known through an electromagnetic counterpart. As shown by

Gürsel and Tinto [20], it is possible to construct a specific linear combination of the outputs of multiple detectors in a network, the *null stream*, which has the property of removing any tensor signal that may be present in the data. This idea was further extended and built on in [21–23]; see also [24, 25] in the context of third-generation detectors such as Einstein Telescope. A commonly used application for LIGO-Virgo gravitational wave searches is X-Pipeline [23, 26], which assumes that only tensor polarizations can be present, and then compares the *null energy* (essentially the square of the null stream) with other combinations of detector outputs to search for GW signals that are in accordance with GR. As pointed out in [19, 27], null streams can also be used to study a signal’s non-tensorial polarization content that may result from a GR violation.

Here we introduce two concrete data analysis pipelines that make use of the fact that if there are only tensor polarizations, the null energy of [23], when evaluated at the true sky position, follows a particular  $\chi^2$  distribution, but not if extra polarizations are present. A first method to discover alternative polarization content then quantifies to what extent the null energy for the given sky position is consistent with this  $\chi^2$  distribution. In a second method the sky position is *a priori* left free, allowing us to turn the tensor-only distribution for the null energy into a probability distribution for the sky location. This sky map will be biased if alternative polarizations are present, which can be quantified by comparing it with the true position of the source on the sky.

Suppose that in a given signal, alternative polarizations are in fact present, mixed with tensor polarizations.

\* [thopang@nikhef.nl](mailto:thopang@nikhef.nl)

† [klllo@caltech.edu](mailto:klllo@caltech.edu)

‡ [cwfong@phy.cuhk.edu.hk](mailto:cwfong@phy.cuhk.edu.hk)

Then to determine the precise nature and relative contributions of the additional modes, in general one would need a network of at least five detectors in addition to the sky position [19, 27, 28].<sup>1</sup> Although in the near future KAGRA [32] will join the discovery efforts, and LIGO-India [33] is about to be built, for now only the two LIGO interferometers and Virgo are making regular detections. However, what we want to establish first of all is whether or not GW signals contain extra polarizations, *irrespective of how much each possible type contributes*, and this is what our two methods enable us to do. If we were to find evidence that GW signals tend to contain more than just tensor polarizations, then this would be a powerful motivation to extend the global detector network even further, in order to be able to study what precisely is contained in a mix of polarizations. Finally, the fact that our methodology is based on the null energy implies that no waveform models are required, so that apart from compact binary coalescences, signals from any transient source (supernovae, cosmic strings, ...) can be studied.

This paper is structured as follows. Sec. II recalls the effects of different polarization modes on interferometric gravitational wave detectors. Sec. III explains our two methods for finding additional polarizations, one based on the null energy for the true sky position, and the other on sky maps. In Sec. IV we perform a simulation whereby signals with a varying amount of scalar polarization in addition to the tensor modes are “injected” into synthetic stationary, Gaussian noise, and we compare the performance of the two analysis pipelines. The methodology is also applied to the binary neutron star signal GW170817, showing consistency with the hypothesis that only tensor polarizations were present. A summary and conclusions are given in Sec. V.

## II. GRAVITATIONAL WAVE POLARIZATIONS

In generic metric theories of gravity, up to six independent polarization modes can be present, namely a breathing mode, a longitudinal mode, the “X” vector mode, the “Y” vector mode, and the usual tensor modes predicted by GR [34]. The effect of different polarization modes on a ring of free-falling test mass is shown in Fig. 1. In all the panels of the figure, a gravitational wave is traveling in the  $z$ -direction. The solid and dotted lines illustrate the deformation of the ring in response to the various modes. Interferometric gravitational wave detectors will react accordingly, with beam pattern functions given by

[34]

$$\begin{aligned} F_B &= -\frac{1}{2} \sin^2 \theta \cos 2\phi, \\ F_L &= \frac{1}{2} \sin^2 \theta \cos 2\phi, \\ F_X &= -\sin \theta (\cos \theta \cos 2\phi \cos \psi - \sin 2\phi \sin \psi), \\ F_Y &= -\sin \theta (\cos \theta \cos 2\phi \sin \psi + \sin 2\phi \cos \psi), \\ F_+ &= \frac{1}{2} (1 + \cos^2 \theta) \cos 2\phi \cos 2\psi - \cos \theta \sin 2\phi \sin 2\psi, \\ F_\times &= \frac{1}{2} (1 + \cos^2 \theta) \cos 2\phi \sin 2\psi + \cos \theta \sin 2\phi \cos 2\psi. \end{aligned} \quad (1)$$

Here  $(\theta, \phi)$  is the sky location of the source, and  $\psi$  is the so-called polarization angle. The subscripts “B”, “L”, “X”, “Y”, “+”, and “ $\times$ ” respectively denote the breathing mode, the longitudinal mode, the X vector mode, the Y vector mode, the “+” tensor polarization, and the “ $\times$ ” tensor polarization. As can be seen from the expressions for  $F_B$  and  $F_L$ , there is a degeneracy between the responses of the two scalar modes; in our analyses we only consider the breathing mode.

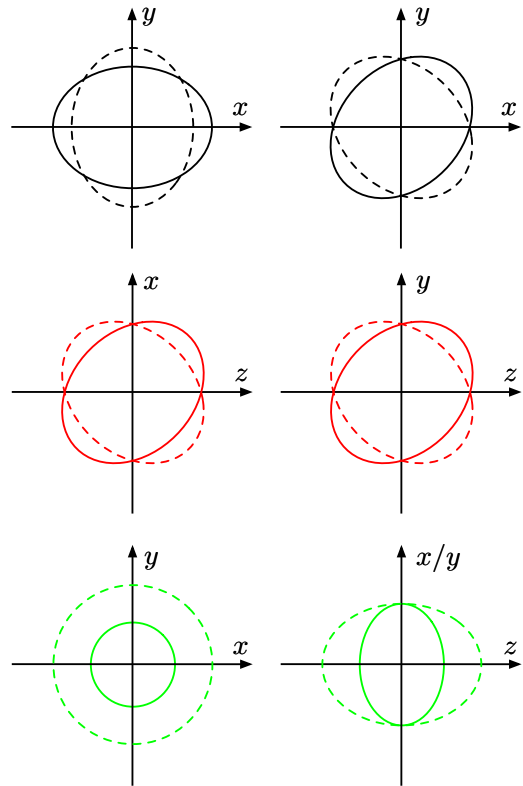


FIG. 1. The effect on a ring of free-falling test particles of a gravitational wave in “+” tensor mode (upper left), “ $\times$ ” tensor mode (upper right), “X” vector mode (middle left), “Y” vector mode (middle right), breathing mode (lower left) and longitudinal mode (lower right). In each case the wave is traveling in the  $z$ -direction. The solid and dotted lines are the states of the ring with a phase difference of  $\pi$ .

<sup>1</sup> An exception occurs for certain special sky positions with respect to the network; see [29–31].

### III. METHODOLOGY

Now consider a *network* of  $D$  gravitational wave detectors labeled by  $\alpha = 0, \dots, D$ , located on the Earth at positions  $\vec{r}_\alpha$  with respect to a geocentric coordinate system, and producing strain outputs  $d_\alpha$ . A gravitational wave is assumed to originate from a source with sky location  $\hat{\Omega} = (\theta, \phi)$ , arriving at the geocenter at a time  $t$ . If only the tensor polarizations are present, one has

$$d_\alpha(t + \Delta t_\alpha) = F_{+, \alpha}(\hat{\Omega})h_+(t) + F_{\times, \alpha}(\hat{\Omega})h_\times(t) + n_\alpha(t + \Delta t_\alpha), \quad (2)$$

where  $F_{\alpha,+}$ ,  $F_{\alpha,\times}$  are the beam pattern functions and  $n_\alpha$  is the noise of detector  $\alpha$ . The time shifts  $\Delta t_\alpha$  are given by

$$\Delta t_\alpha = \frac{\vec{r}_\alpha}{c} \cdot (-\hat{\Omega}). \quad (3)$$

We can write the  $D$ -detector observation model more compactly in matrix form:

$$\mathbf{d} = \mathbf{F}\mathbf{h} + \mathbf{n}, \quad (4)$$

where

$$\mathbf{d} = \begin{pmatrix} d_0 \\ \vdots \\ d_{D-1} \end{pmatrix}, \quad \mathbf{h} = \begin{pmatrix} h_+ \\ h_\times \end{pmatrix}, \quad \mathbf{n} = \begin{pmatrix} n_0 \\ \vdots \\ n_{D-1} \end{pmatrix}, \quad (5)$$

and

$$\mathbf{F} = (\mathbf{F}_+ \quad \mathbf{F}_\times) = \begin{pmatrix} F_{+,0} & F_{\times,0} \\ \vdots & \vdots \\ F_{+,D-1} & F_{\times,D-1} \end{pmatrix}. \quad (6)$$

#### A. Null energy

In the above, the gravitational wave signal  $\mathbf{s} = \mathbf{F}\mathbf{h}$  can be viewed as being in a subspace of the space of detector outputs spanned by  $\mathbf{F}_+$  and  $\mathbf{F}_\times$ . We can construct the *null projector*  $\mathbf{P}_{\text{null}}(\hat{\Omega})$  [26], which projects away the signal when the projector is constructed with the true sky location. The null projector is given by

$$\mathbf{P}_{\text{null}} = \mathbf{I} - \mathbf{F}_w(\mathbf{F}_w^\dagger \mathbf{F}_w)^{-1} \mathbf{F}_w^\dagger, \quad (7)$$

where  $\dagger$  denotes Hermitian conjugation and  $\mathbf{F}_w$  are the noise-weighted beam pattern functions [26]. If we apply the null projector with the true sky location on the strain data in Eq. 4, we obtain

$$\begin{aligned} \tilde{\mathbf{z}}(\hat{\Omega}_{\text{true}}) &= \mathbf{P}_{\text{null}}(\hat{\Omega}_{\text{true}})\tilde{\mathbf{d}}_w \\ &= \mathbf{P}_{\text{null}}(\hat{\Omega}_{\text{true}})\mathbf{F}_w(\hat{\Omega}_{\text{true}})\tilde{\mathbf{h}} + \mathbf{P}_{\text{null}}(\hat{\Omega}_{\text{true}})\tilde{\mathbf{n}}_w \\ &= \mathbf{P}_{\text{null}}(\hat{\Omega}_{\text{true}})\tilde{\mathbf{n}}_w \end{aligned} \quad (8)$$

where  $\tilde{\mathbf{z}}$  is the *null stream* which only consists of noise living in a subspace that is orthogonal to the one spanned by  $\mathbf{F}_{+,w}$  and  $\mathbf{F}_{\times,w}$ , and  $w$  indicates whitening.

In practice, the data are first whitened before applying the null projector. As in [26] we perform the analysis in the time-frequency domain, but using the Wilson-Daubechies-Meyer (WDM) time-frequency transform because of its superior time-frequency localization [35]. The *null energy* is then defined as [26]

$$\begin{aligned} E_{\text{null}} &= \sum_k \tilde{\mathbf{z}}_w^\dagger \tilde{\mathbf{z}}_w \\ &= \sum_k \tilde{\mathbf{d}}_w^\dagger \mathbf{P}_{\text{null}}^\dagger \mathbf{P}_{\text{null}} \tilde{\mathbf{d}}_w \\ &= \sum_k \tilde{\mathbf{d}}_w^\dagger \mathbf{P}_{\text{null}} \tilde{\mathbf{d}}_w, \end{aligned} \quad (9)$$

where  $w$  indicates whitening, a tilde refers to the data matrix resulting from the WDM transform, and  $\sum_k$  sums over the discrete time-frequency pixels. The quantity  $E_{\text{null}}$  follows a  $\chi^2$  distribution with  $\text{DoF} = N_{\tau f}(D - 2)$  degrees of freedom, where  $N_{\tau f}$  is the number of time-frequency pixels used in the analysis.<sup>2</sup>

Now let us assume that there is polarization content in the signal beyond the tensor polarizations. The whitened data matrix can then be written as

$$\tilde{\mathbf{d}}_w = \mathbf{F}_{w,t}\tilde{\mathbf{h}}_t + \mathbf{F}_{w,e}\tilde{\mathbf{h}}_e + \tilde{\mathbf{n}}_w, \quad (10)$$

where the index  $t$  is summed over  $+$  and  $\times$ , while the index  $e$  is summed over whatever additional polarizations are present. The null energy calculated at the source's location with pure-tensor beam pattern matrix is given by

$$\begin{aligned} E_{\text{null}} &= \sum_k \tilde{\mathbf{d}}_w^\dagger \mathbf{P}_{\text{null}} \tilde{\mathbf{d}}_w \\ &= \sum_k \tilde{\mathbf{n}}_w^\dagger \mathbf{P}_{\text{null}} \tilde{\mathbf{n}}_w + \sum_k \tilde{\mathbf{h}}_e^\dagger \mathbf{F}_{e,w}^\dagger \mathbf{P}_{\text{null}} \mathbf{F}_{e',w} \tilde{\mathbf{h}}_{e'} \\ &\quad + \sum_k 2\Re(\tilde{\mathbf{h}}_e^\dagger \mathbf{F}_{e,w}^\dagger \mathbf{P}_{\text{null}}^t \tilde{\mathbf{n}}_w), \end{aligned} \quad (11)$$

where the last two terms signify the presence of the extra polarizations. Next we explain how the  $\chi^2$  distribution which the null energy would follow in the absence of these additional polarizations, can be used to detect them, in two different ways.

#### B. Null energy method and sky map method

As mentioned before, we assume gravitational wave events with electromagnetic counterpart, so that the true

---

<sup>2</sup> Note that in [26], DoF has an extra prefactor 2, which is not present here because the WDM coefficients are real.

sky position  $\hat{\Omega}_{\text{true}}$  is known. With the null energy formalism of the previous subsection, this leads to two methods for establishing whether alternative polarizations are present.

- If there are additional polarizations in the signal, then the null energy evaluated at  $\hat{\Omega}_{\text{true}}$  will no longer follow the  $\chi^2$  distribution described above. To quantify the size of the deviation, we can assign a p-value to the hypothesis that only tensor polarizations are present, given by

$$p = 1 - \int_0^{E_{\text{null}}} \chi_{\text{DoF}}^2(x) dx. \quad (12)$$

A small p-value indicates a strong appearance of the additional terms in the right hand side of Eq. (11), suggesting a deviation from GR. In the sequel this method will simply be referred to as the *null energy method*.

- Alternatively, in the definition (9) for the null energy one can leave  $\hat{\Omega}$  free. This leads to a sky map, or probability distribution for  $\hat{\Omega}$  through  $\mathcal{P}(\hat{\Omega}) \equiv \chi_{\text{DoF}}^2(E_{\text{null}}(\hat{\Omega}))$ . If additional polarizations are in fact present in the signal, then they will cause systematics in  $\mathcal{P}(\hat{\Omega})$  due to the detectors' responses to them. The true sky location  $\hat{\Omega}_{\text{true}}$  will fall on the boundary of some  $(1 - q)$  credible interval, where  $q$  is given by

$$q = \int d\hat{\Omega} \mathcal{P}(\hat{\Omega}) H(\mathcal{P}(\hat{\Omega}_{\text{True}}) - \mathcal{P}(\hat{\Omega})), \quad (13)$$

with  $H(x)$  the Heaviside step function. The quantity  $q$  can then be interpreted as a p-value for the tensor-only hypothesis. In what follows this method will be referred to as the *sky map method*.

Both methods allow us to combine information from multiple sources so as to arrive at a stronger statement on the validity of GR, or lack thereof. If GR is an accurate description of the gravitational wave polarization, then the values of  $p$  obtained from the null energy method and the values of  $q$  obtained using the sky map method should be distributed uniformly between 0 and 1. As shown by Fisher [36], if one has  $N$  samples  $\{q_i\}$  following a uniform distribution between 0 and 1, the test statistic  $S$  given by

$$S = -2 \sum_{i=1}^N \log(q_i), \quad (14)$$

follows a  $\chi^2$  distribution with  $2N$  degrees of freedom. Therefore, the combined p-value  $p_{\text{com}}$  is given by

$$p_{\text{com}} = 1 - \int_0^S \chi_{2N}^2(x) dx. \quad (15)$$

In what follows, we first test the two methods through an extensive simulation, and then apply them to the binary neutron star signal GW170817.

#### IV. SIMULATIONS, AND ANALYSES OF GW170817

In this section we evaluate the performance of the null stream and sky map methods by “injecting” simulated signals into synthetic Gaussian, stationary noise following predicted noise power spectral densities for Advanced LIGO and Advanced Virgo at their respective design sensitivities. We take the sources to be zero-spin binary neutron star inspirals with component masses uniformly distributed in  $[1, 2] M_\odot$ . Positions in the Universe are distributed uniformly in co-moving volume, with a network signal-to-noise threshold of 12. Binary neutron stars are chosen because of their ability to generate electromagnetic counterpart when they merge, but in principle other transient sources could be considered.

To test the sensitivities of our methods, apart from simulated signals that follow GR we also inject sets of mock scalar-tensor waveforms. The scalar component  $h_S$  of the latter signals is taken to be

$$h_S(t) = \mathcal{A}_S^T h_T(t; \text{with a } \pi/4 \text{ phase shift}), \quad (16)$$

where  $h_T(t)$  equals  $h_+(t)$  at zero inclination, and the  $\pi/4$  phase shift is a strawman for the more general ways in which the time evolution of the scalar component might differ from that of the tensor components in various alternative theories [19]. In each of four sets of scalar-tensor injections we let the scalar-to-tensor ratio  $\mathcal{A}_S^T$  take values of 0.25, 0.5, 0.75, or 1.0.

Fig. 2 shows  $\log_{10}$  of the combined p-value  $p_{\text{com}}$  calculated with the skymap method and the null energy method against the number of events. Even for  $\mathcal{A}_S^T = 0.25$ , it takes only a few tens of detections with electromagnetic counterparts to establish a  $5\sigma$  violation of GR. Comparatively, the null energy method shows a higher sensitivity since it requires fewer events to attain the  $5\sigma$  level.

We note that  $p_{\text{com}}$  for GR signals gradually approaches the  $5\sigma$  line as the number of events increases; this is because of the systematics in the clustering algorithm used. The largest high power cluster is consistently selected to be the event candidate, but there is a non-negligible chance for high power noise pixels to be included in the periphery of the cluster. This happens especially when the burst energy of the signal is not significantly higher than the background noise. The systematic error accumulates as the number of events increases. Hence, when analyzing real data, we will have to inject large numbers of simulated GR signals into real noise to obtain a reference or “background” distribution of the test statistic to compare “foreground” results with. This procedure will automatically account for the non-stationary and non-

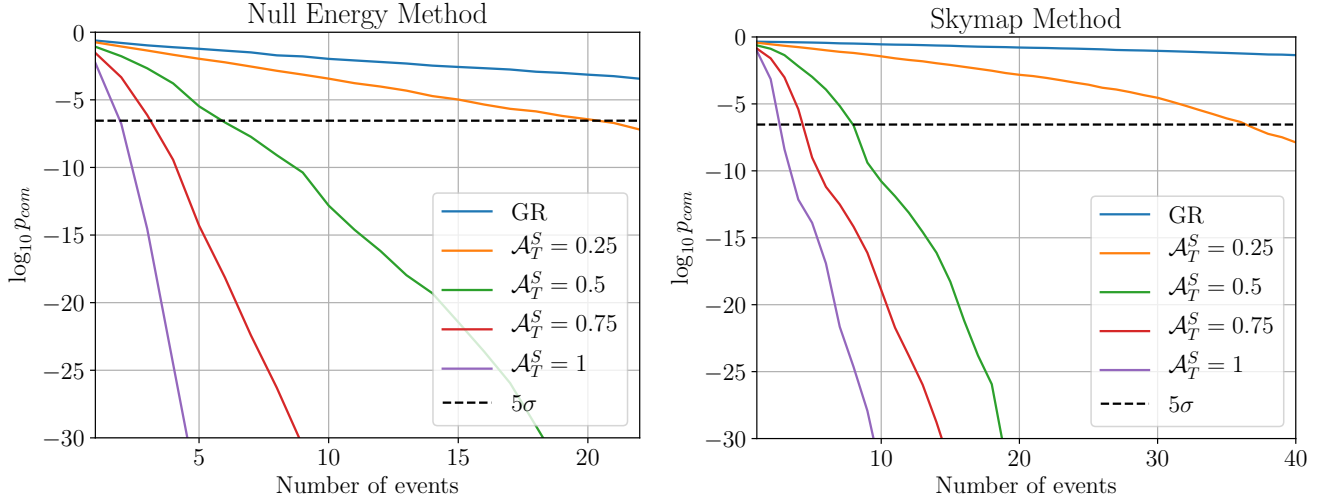


FIG. 2.  $\log_{10}$  of combined p-values with null energy method (left panel) and skymap method (right panel) against the number of combined events, both for the GR case and for different sets of mock scalar-tensor signals as described in the main text. For all sets of non-GR injections, GR can be rejected at the  $5\sigma$  level with a few to a few tens of detections.

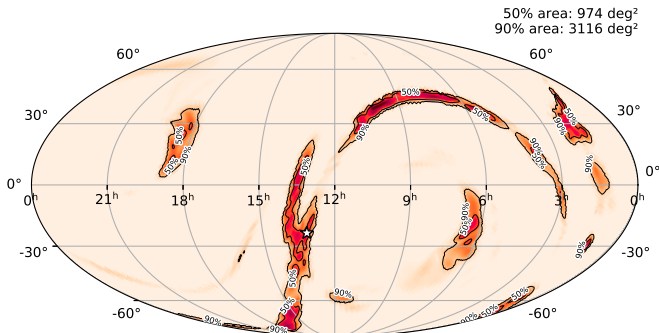


FIG. 3. Sky map  $\mathcal{P}(\hat{\Omega})$  for GW170817. The star indicates the sky location of the corresponding counterpart SSS17a/AT 2017gfo [37]. The sky map is consistent with the counterpart location, which is enclosed in the 50% confidence contour.

Gaussian nature of detector noise as well as the systematics due to the clustering method.

These results show that our analysis pipelines are capable of testing the existence of alternative polarization modes in addition to tensor modes with a 3-detector network. Given a few tens of detections with known sky position, both methods are sensitive to a scalar mode whose amplitude is a quarter of that of the tensor mode.

A binary neutron star coalescence GW170817 was observed on 17 August 2017 with merger time 12:41:04 UTC (or GPS time 1187008882.4457) [8, 38, 39]. Electromagnetic counterparts were seen, and in particular an optical counterpart was found with very precise localization at right ascension and declination  $\alpha = 13^{\text{h}}09^{\text{m}}48^{\text{s}}.085 \pm 0.018$  and  $\delta = -23^{\circ}22'53''.343 \pm 0.218$ , respectively [40], which provides us an opportunity to apply our tests for

alternative polarizations. The null energy test yields a p-value of 0.315, while the sky map method gives 0.790; in the latter case, the sky map  $\mathcal{P}(\hat{\Omega})$  and true sky location  $\hat{\Omega}_{\text{true}}$  are shown in Fig. 3. Hence, both tests indicate consistency with the tensor-only hypothesis.

## V. SUMMARY AND CONCLUSIONS

We have introduced two methods to search for polarization modes in addition to the tensor modes, which can be used even with a limited network of detectors (e.g. the two LIGOs and Virgo), though an identifiable electromagnetic counterpart is needed. Both formalisms are based on the notion of null energy. In one case (the *null energy test*) we use the statistical distribution of the null energy for the given true sky location to compute p-values for the validity of the tensor-only hypothesis. The other method (the *sky map test*) first leaves the sky location to be free, turning the distribution of null energy into a sky map, for which the consistency with the true sky location can again be quantified in terms of a p-value. Apart from being able to detect mixtures of different polarization modes rather than having to consider purely tensor, purely vector, and purely scalar hypotheses, no waveform models are needed, so that any transient gravitational wave signal can be used in the tests.

By injecting mock scalar-tensor signals into synthetic stationary and Gaussian noise, we illustrated how both tests can find scalar contributions at  $5\sigma$  confidence with a few tens of signals that have electromagnetic counterparts if the scalar contribution in each signal is at the 25% level. The null energy test turns out to be slightly more sensitive than the skymap method. Both methods

show a slowly accumulating bias towards a GR violation when applied to pure tensor signals, due to the null energy clustering algorithm picking up high-energy noise pixels. Thus there is scope for improvement, although even if tens of signals with counterparts were available today, we would certainly be able to already use either method by constructing a reference distribution for our detection statistic and compare “foreground” results with this “background” distribution.

Finally, we have applied our methods to GW170817, finding consistency with the pure-tensor hypothesis. To our knowledge this is the first time a search for a mixture of gravitational wave polarizations has been performed.

## ACKNOWLEDGMENTS

PTHP and CVDB are supported by the research program of the Netherlands Organization for Scientific Research (NWO). TGFL and ICFW are partially supported by grants from the Research Grants Council of the Hong Kong (Project No. 24304317 and 14306419), Research Committee of the Chinese University of Hong Kong and the Croucher Foundation of Hong Kong. RKLL and TGFL would also like to gratefully acknowledge the support from the Croucher Foundation in Hong Kong.

This research has made use of data, software and/or web tools obtained from the Gravitational Wave Open Science Center (<https://www.gw-openscience.org>), a service of LIGO Laboratory, the LIGO Scientific Collaboration and the Virgo Collaboration. LIGO is funded by the U.S. National Science Foundation. Virgo is funded by the French Centre National de Recherche Scientifique (CNRS), the Italian Istituto Nazionale della Fisica Nucleare (INFN) and the Dutch Nikhef, with contributions by Polish and Hungarian institutes.

- 
- [1] J. Aasi *et al.* (LIGO Scientific), *Class. Quant. Grav.* **32**, 074001 (2015), arXiv:1411.4547 [gr-qc].
  - [2] F. Acernese *et al.* (VIRGO), *Class. Quant. Grav.* **32**, 024001 (2015), arXiv:1408.3978 [gr-qc].
  - [3] B. P. Abbott (2017) pp. 291–311.
  - [4] B. P. Abbott *et al.* (Virgo, LIGO Scientific), *Phys. Rev. Lett.* **116**, 241103 (2016), arXiv:1606.04855 [gr-qc].
  - [5] B. P. Abbott *et al.* (Virgo, LIGO Scientific), *Phys. Rev. X* **6**, 041015 (2016), arXiv:1606.04856 [gr-qc].
  - [6] B. P. Abbott *et al.* (VIRGO, LIGO Scientific), *Phys. Rev. Lett.* **118**, 221101 (2017), arXiv:1706.01812 [gr-qc].
  - [7] B. P. Abbott *et al.* (Virgo, LIGO Scientific), *Astrophys. J.* **851**, L35 (2017), arXiv:1711.05578 [astro-ph.HE].
  - [8] B. P. Abbott, R. Abbott, T. D. Abbott, F. Acernese, *et al.* (LIGO Scientific Collaboration and Virgo Collaboration), *Phys. Rev. Lett.* **119**, 161101 (2017).
  - [9] B. P. Abbott *et al.* (Virgo, LIGO Scientific), *Phys. Rev. Lett.* **119**, 141101 (2017), arXiv:1709.09660 [gr-qc].
  - [10] B. P. Abbott *et al.* (LIGO Scientific, Virgo), (2018), arXiv:1811.12907 [astro-ph.HE].
  - [11] B. P. Abbott *et al.* (LIGO Scientific, Virgo), (2020), arXiv:2001.01761 [astro-ph.HE].
  - [12] B. P. Abbott *et al.* (Virgo, LIGO Scientific), *Phys. Rev. Lett.* **116**, 221101 (2016), arXiv:1602.03841 [gr-qc].
  - [13] B. P. Abbott *et al.* (Virgo, LIGO Scientific), *Phys. Rev. X* **6**, 041015 (2016), arXiv:1606.04856 [gr-qc].
  - [14] B. P. Abbott *et al.* (LIGO Scientific, Virgo), (2019), arXiv:1903.04467 [gr-qc].
  - [15] B. P. Abbott *et al.* (LIGO Scientific, Virgo), (2018), arXiv:1811.00364 [gr-qc].
  - [16] B. P. Abbott *et al.* (LIGO Scientific, Virgo, Fermi-GBM, INTEGRAL), *Astrophys. J.* **848**, L13 (2017), arXiv:1710.05834 [astro-ph.HE].
  - [17] M. Isi and A. J. Weinstein, (2017), arXiv:1710.03794 [gr-qc].
  - [18] D. M. Eardley, D. L. Lee, and A. P. Lightman, *Phys. Rev. D* **8**, 3308 (1973).
  - [19] K. Chatzioannou, N. Yunes, and N. Cornish, *Phys. Rev. D* **86**, 022004 (2012).
  - [20] Y. Gürsel and M. Tinto, *Phys. Rev. D* **40**, 3884 (1989).
  - [21] L. Wen and B. F. Schutz, *Gravitational wave data analysis. Proceedings, 9th Workshop, GWDW 2004, Annecy, France, December 15–18, 2004*, *Class. Quant. Grav.* **22**, S1321 (2005), arXiv:gr-qc/0508042 [gr-qc].
  - [22] P. Ajith, M. Hewitson, and I. S. Heng, *Gravitational wave data analysis. Proceedings, 10th Workshop, GWDW-10, Brownsville, USA, December 14–17, 2005*, *Class. Quant. Grav.* **23**, S741 (2006), arXiv:gr-qc/0604004 [gr-qc].
  - [23] S. Chatterji, A. Lazzarini, L. Stein, P. J. Sutton, A. Searle, and M. Tinto, *Phys. Rev. D* **74**, 082005 (2006), arXiv:gr-qc/0605002 [gr-qc].
  - [24] A. Freise, S. Chelkowski, S. Hild, W. Del Pozzo, A. Perreca, and A. Vecchio, *Class. Quant. Grav.* **26**, 085012 (2009), arXiv:0804.1036 [gr-qc].
  - [25] T. Regimbau *et al.*, *Phys. Rev. D* **86**, 122001 (2012), arXiv:1201.3563 [gr-qc].
  - [26] P. J. Sutton, G. Jones, S. Chatterji, P. Kalmus, I. Leonor, S. Poprocki, J. Rollins, A. Searle, L. Stein, M. Tinto, and M. Was, *New Journal of Physics* **12**, 053034 (2010), arXiv:0908.3665 [gr-qc].
  - [27] K. Hayama and A. Nishizawa, *Phys. Rev. D* **87**, 062003 (2013), arXiv:1208.4596 [gr-qc].
  - [28] C. Van Den Broeck, in *Springer Handbook of Spacetime*, edited by A. Ashtekar and V. Petkov (2014) pp. 589–613, arXiv:1301.7291 [gr-qc].
  - [29] Y. Hagihara, N. Era, D. Iikawa, and H. Asada, *Phys. Rev. D* **98**, 064035 (2018), arXiv:1807.07234 [gr-qc].
  - [30] Y. Hagihara, N. Era, D. Iikawa, A. Nishizawa, and H. Asada, *Phys. Rev. D* **100**, 064010 (2019), arXiv:1904.02300 [gr-qc].
  - [31] Y. Hagihara, N. Era, D. Iikawa, N. Takeda,

- and H. Asada, *Phys. Rev.* **D101**, 041501 (2020), arXiv:1912.06340 [gr-qc].
- [32] Y. Aso *et al.* (KAGRA), *Phys. Rev.* **D88**, 043007 (2013), arXiv:1306.6747 [gr-qc].
- [33] B. Iyer *et al.*, *LIGO India*, Tech. Rep. LIGO-M1100296 (2011) <https://dcc.ligo.org/LIGO-M1100296/public>.
- [34] E. Poisson and C. M. Will, *Gravity: Newtonian, Post-Newtonian, Relativistic* (Cambridge University Press, 2014).
- [35] V. Necula, S. Klimenko, and G. Mitselmakher, *Journal of Physics: Conference Series* **363**, 012032 (2012).
- [36] R. A. Fisher, *Statistical methods for research workers*. *Fourteenth Edition Revised* (Oliver and Boyd, 1970).
- [37] B. P. Abbott *et al.* (LIGO Scientific, Virgo), *Phys. Rev.* **X9**, 011001 (2019), arXiv:1805.11579 [gr-qc].
- [38] LIGO Scientific Collaboration and Virgo Collaboration, <https://www.gw-openscience.org/events/GW170817/> (2017).
- [39] M. Vallisneri, J. Kanner, R. Williams, A. Weinstein, and B. Stephens, *Journal of Physics: Conference Series* **610**, 012021 (2015).
- [40] B. P. Abbott *et al.*, *The Astrophysical Journal* **848**, L12 (2017).